European Journal of Pharmaceutics and Biopharmaceutics 142 (2019) 449–459

Contents lists available at ScienceDirect

European Journal of Pharmaceutics and Biopharmaceutics

journal homepage: www.elsevier.com/locate/ejpb

Research paper

Versatile protamine nanocapsules to restore miR-145 levels and interfere tumor growth in colorectal cancer cells

Sonia Reimondez-Troitiño[a,b], José V. González-Aramundiz[b,c], Juan Ruiz-Bañobre[a], Rafael López-López[a], María J. Alonso[b], Noemi Csaba[b,*], María de la Fuente[a,*]

[a] Nano-Oncology Unit, Translational Medical Oncology Group, Health Research Institute of Santiago de Compostela (IDIS), Clinical University Hospital of Santiago de Compostela (CHUS), CIBERONC, Santiago de Compostela, Spain
[b] Center for Research in Molecular Medicine and Chronic Diseases (CIMUS), Department of Pharmacy and Pharmaceutical Technology, School of Pharmacy, University of Santiago de Compostela, Campus Vida, Santiago de Compostela, Spain
[c] Departamento de Farmacia, Facultad de Química y de Farmacia, Pontificia Universidad Católica de Chile, 7820436 Santiago, Chile

ARTICLE INFO

Keywords:
Protamine nanocapsules
Gene therapy
microRNAs
miR-145
Curcumin
Colorectal cancer

ABSTRACT

MicroRNAs (miRNAs) play a key role on gene expression regulation contributing to cell homeostasis, and they are highly dysregulated in cancer. Consequently, miRNA-based therapies are an attractive approach to develop novel anticancer strategies. The main objective of this work was to explore the full potential of protamine nanocapsules (Pr NCs) to develop an anticancer therapy based on the restoration of oncosuppressor miR-145, downregulated in colorectal cancer cells. The composition of Pr NCs was defined based on the selection of surfactants, and protamine that would enable an efficient association and intracellular delivery of miRNA mimics according to the layer-by-layer approach, and the encapsulation of curcumin within the oily core. After exposure of colorectal cancer cells with (i) miR-145 and (ii) curcumin-loaded Pr NCs, a strong increase in the intracellular levels of miR-145, which translated into a decreased cell proliferation rate and migration capacity of the treated cells, was observed. The potential of exploiting Pr NCs for the co-delivery of both biomolecules, miRNAs and curcumin, has also been proved. All together, here we evaluate the possibility to use Pr NCs to efficiently increase the intracellular levels of the oncosuppressor miR-145.

1. Introduction

Colorectal cancer is considered the third most common cancer worldwide. The global burden of the disease is expected to increase to more than 2.2 million new cases and 1.1 million cancer-related deaths by 2030 [1,2]. Poor patient survival is directly attributable to widespread metastasis, drug resistance, and the lack of effective treatment strategies. Indeed, although survival for earlier stages has significantly improved in the last years, colorectal cancer continuous to be a devastating disease in the metastatic setting. The design of innovative therapies against specific intracellular targets can provide alternatives for interfering tumor proliferation and dissemination.

The increasing understanding on the role of microRNAs (miRNAs) in cell homeostasis and disease, especially in cancer, has unveiled their therapeutic potential [3–7]. miRNA levels can be precisely upregulated through the use of miRNA mimics. In addition, their levels can also be indirectly modulated by natural compounds such as curcumin [8,9].

miR-145 is downregulated in several types of cancer and several authors have shown how miR-145 replacement therapies based on viral vectors or commercial transfecting reagents (i.e. Lipofectamine®), reduce tumor growth, migration, and prevent drug resistance both *in vitro* and *in vivo*. These examples include prostate cancer [10], colon cancer [11,12], breast cancer [13], and bladder cancer [14], among others. Nevertheless, clinical translation of such strategies depends on the development of efficient and safe delivery systems [15]. Cationic liposomes (made of DOTAP/cholesterol and protamine), cationic complexes (based on PLGA/PEI/HA, PEI, or Polyurethanes/PEI), lipid-based nanoparticles, and iron oxide magnetic nanoparticles, have already been proposed for the delivery of oncosuppressor miRNAs, either as miRNA mimics [16,17], or as plasmid vectors encoding miRNAs [18–22].

Curcumin, a polyphenol obtained from turmeric, has been widely investigated for its interesting biological properties (anticancer, anti-inflammatory, antioxidant, hypolipidaemic, antiviral, and antibacterial activities [23–25]). Anticancer effects of curcumin have been reported for breast, cervical, prostate and colorectal cancer, as recently reviewed

* Corresponding authors.
E-mail addresses: noemi.csaba@usc.es (N. Csaba), maria.de.la.fuente.freire@sergas.es (M. de la Fuente).

https://doi.org/10.1016/j.ejpb.2019.07.016
Received 13 April 2019; Received in revised form 28 June 2019; Accepted 15 July 2019
Available online 18 July 2019
0939-6411/ © 2019 Elsevier B.V. All rights reserved.

[24]. Curcumin exert its chemotherapeutic activity by inducing apoptosis, inhibiting proliferation, migration and invasion of cancer cells, sensitizing tumors to radiotherapy and chemotherapy [26], and also modulating the expression of miRNAs [8,9]. At a molecular level, curcumin has been shown to suppress a number of cell signaling pathways including PI3K/Akt/mTOR [24] and IGF-1R signaling [24,27]. However, its formulation in an injectable form possess problems related to its poor stability and water solubility [28]. Nano-sized drug delivery systems represent a promising strategy to overcome these limitations. Previous attempts to deliver curcumin to U87MG cells and increase the intracellular miR-145 levels have made use of a dendrosomal formulation, containing PEG400 and oleoyl chloride [29], as well as chitosan and PEG/PLGA nanoparticles [30,31].

Protamine nanocapsules (Pr NCs) composed by an oily core and a protamine shell, were initially developed in our lab for the delivery of proteins and vaccines [32,33]. Based on the capacity of protamine to condense nucleic acids and facilitate their translocation across the cell membrane [18,34–38], we have taken the challenge to associate a miRNA mimics, miR-145, to the protamine shell, and to encapsulate curcumin within the oily core. Importantly, simultaneous association of these two biomolecules, having different physicochemical properties, have also been achieved. To assess the potential of Pr NCs, we have investigated the capacity of this novel formulations to restore intracellular miR-145 and mediate an anti-proliferative and anti-migratory effect.

2. Experimental section

2.1. Materials

Protamine sulphate (Mw 5KDa) was obtained from Yuki Gosei Kogyo Co., Ltd (Tokyo, Japan). Sodium hyaluronate (Mw 57 KDa) was purchased from Lifecore Biomedical (Chaska, MN, USA). Agarose, 3-(4,5-dimethylthiazol-2-yl)-5-(3-carboxymethoxyphenyl)-2-(4-sulfophenyl)-2H-tetrazolium (MTT), D-α-tocopheryl polyethyleneglycol 1000 succinate (TPGS), Triton-X, cell culture media Dulbecco's Modified Eagle's Medium (DMEM), and heparin were purchased from Sigma Aldrich (Madrid, Spain). Sodium cholate was obtained from Dext1a (Reading, UK). Tween® 80 (T80) was acquired from Acofarma (Madrid, Spain). PEG-stearate (Simulsol® M52) was obtained from Seppic, (Paris, France). DL-α-tocopherol (vitamin E) was purchased from Merck (Darmstad, Germany). 5-Carboxy tetramethyl rhodamine succinimidyl ester (5-TAMRA) was from EMP Biotech (Berlin, Germany). Curcumin was purchased in Axxora (Madrid, Spain). RNAs were purchased from Eurofins MWG Operon (Ebersberg, Germany) (Cy5-modified RNA: 5′ Cy5-AGGUAGUGUAAUCGCCUUG 3′; miRNA scramble (miRNA-scr): 5′ UUCUCCGAACGUUGUCACGUUU 3′; miR-145: 5′ GUCCAGUUUUCCCAGGAAUCCCU 3′). SYBR®Gold Nucleic Acid Gel Stain, penicillin and streptomycin were acquired from Invitrogen (Madrid, Spain). The solvents, ethanol and acetone, were of analytical grade and obtained from Thermo Fisher Scientific (Madrid, Spain). Ultrapure Milli-Q water was used all throughout the experiments.

2.2. Preparation of protamine nanocapsules

Pr NCs were prepared by the solvent displacement technique, following the procedure previously described by our group [39]. For that purpose, we have selected different surfactants. In brief, nanocapsules were prepared with sodium cholate (5 mg, or 4 mg in the case of the formulation with T80), in combination with (i) PEG-stearate (PEG-st) (12 mg), (ii) TPGS (12 mg), or (iii) T80 (8 mg). The oil was, in all cases, vitamin E (60 mg, or 50 mg in the case of the formulation with T80). The oil and surfactants were dissolved in 0.750 mL of ethanol, followed by the addition of 4.25 mL of acetone. This organic phase was immediately poured over 10 mL of an aqueous solution containing 5 mg of protamine. The elimination of organic solvents was performed by evaporation under vacuum (Rotavapor Heidolph, Germany), to a constant volume of 5 mL. Thereafter, protamine nanocapsules were isolated by ultracentrifugation (OptimaTM L-90 K Ultracentrifugue Beckam Coulter, Rotor type 70.1 Ti, 30,000 rpm, 1 h, 15 °C), obtaining a cream consisting of the isolated Pr NCs on top of the aqueous phase. This aqueous phase was removed and isolated nanocapsules were resuspended to a final volume of 5 mL with ultrapure water.

2.3. Association of nucleic acids to protamine nanocapsules

0.2 mL of isolated Pr NCs were incubated at room temperature with 0.05 mL of a solution of nucleic acids at different concentrations, to obtain theoretical loadings ranging from 1 to 5% in the case of pDNA and 1.5% for miRNA with respect to the total mass of the nanocapsules (w/w). The mixture was left under magnetic stirring for 1 h in order to allow its stabilization. The association of pDNA and miRNA was observed by agarose gel electrophoresis (1 and 2% w/v in Tris-Acetate-EDTA (TAE) Buffer, respectively). 1 μg of pDNA/miRNA labeled with SYBR®Gold, either in solution, associated to the nanocapsules, or after displacement with an excess of heparin (25-fold heparin with respect to the amount of pDNA/miRNA for 2 h at 37 °C) were loaded into each well. The gel was run for 30 min at 90 V in a Sub-Cell GT cell 96/192 (Bio-Rad Laboratories Ltd., England) and imaged with a Molecular Imager® Gel Doc™ XR System (UV light 302 nm; Bio-Rad, Madrid; Spain).

2.4. Layer-by-layer coating of miR-145-loaded protamine nanocapsules

miR-145-loaded Pr NCs were coated with an external layer of protamine upon addition of 0.2 mL of an aqueous solution containing 0.034 mg of protamine to an equal volume of miRNA-loaded Pr NCs, at room temperature under magnetic stirring for 20 min.

2.5. Encapsulation of curcumin within protamine nanocapsules

The encapsulation of curcumin was performed as previously described [40]. In brief, specific volumes of a solution of curcumin in ethanol (1 mg/mL) were incorporated to the organic phase in order to obtain theoretical drug loadings of 0.75 and 2.2% with respect to the total amount of components (w/w). The amount of free drug was determined in the remaining aqueous phase, after ultracentrifugation and separation of the nanocapsules, by fluorescence spectroscopy (EnVision®, λex 420 nm, λem 535 nm, PerkinElmer; USA). Encapsulation efficiencies (EE %) were calculated according to Eq. (1).

$$EE(\%) = (\text{Total curcumin} - \text{Free curcumin in the aqueous phase}) / (\text{Total curcumin}) \times 100 \quad (1)$$

Additionally, miR-145 was also associated to Pr NCs having a curcumin loading of 0.75% (w/w). 0.05 mL of a solution of miR-145, at a concentration of 0.54 mg/mL, were poured over 0.2 mL of curcumin-loaded Pr NCs and incubated for 1 h at room temperature, under magnetic stirring.

2.6. Physicochemical characterization of the nanocapsules

Average particle size and polydispersity index of the developed nanocapsules were determined by photon correlation spectroscopy (Zetasizer Nano-ZS™, Malvern Instruments, England), after sample dilution with ultrapure water. Each analysis was performed in triplicate, at 25 °C and with a scattering angle of 173°. The zeta potential, a parameter indicative of the surface charge of the nanocapsules, was measured by laser doppler anemometry (Zetasizer Nano-ZS™, Malvern Instruments, England), upon dilution in ultrapure water. The yield of production (w/w) of Pr NCs was also determined. For this purpose, isolated Pr NCs were first frozen without any cryoprotectant at – 80 °C

for at least 2 h, and then freeze-dried (GenesisTM 25 EL, S.P. Industries, USA). Lyophilization was done at a temperature ranging from −40 °C to +20 °C, applying a progressive vacuum from 200 mTorr to 20 mTorr. After this process, freeze-dried nanocapsules were directly weighed to calculate the production yield by mass differences according to Eq. (2).

$$\text{Yield } (\%) = (\text{Nanocapsulesweight/Total solid weight}) \times 100 \quad (2)$$

Morphological examination was carried out by transmission electron microscopy (TEM, CM12 Philips; The Netherlands). Samples of the nanocapsules were placed on a copper grid, stained with a solution of phosphotungstic acid 2% (w/v) and vacuum dried overnight before observation.

2.7. Stability of protamine nanocapsules

The stability of Pr NCs in suspension was monitored by the evolution of particle size at 4 °C as an aqueous suspension for up to 1 month and also upon dilution (1/10, v/v) in relevant physiological media (phosphate buffer at pH 7.4 and DMEM supplemented with 10% (v/v) fetal bovine serum (FBS)) and incubation under horizontal shaking at 37 °C, for 7 h. Particle size analysis was carried out as previously described.

2.8. In vitro experiments

SW480 colorectal cancer cells were cultured in DMEM supplemented with 10% v/v) of FBS and 1% (v/v) of penicillin-streptomycin at 37 °C in a humidified atmosphere containing 5% carbon dioxide. All *in vitro* studies were carried out in this media and, using isolated Pr NCs.

2.9. Cytotoxicity studies

1×10^4 SW480 cells were seeded in 96-well plates (0.1 mL/well) and incubated for 24 h, prior to experiment. Different concentrations of isolated protamine nanocapsules (from 0.1 to 2.2 mg/mL) were incubated with cells. Cells incubated with Triton X-100 at 0.1 mg/mL were used as positive control, and untreated cells, as negative control. After 4 h of incubation, the medium was removed and replaced with fresh cell culture medium. The cells were allowed to grow for 96 h in normal conditions. Then, the medium was removed and 0.11 mL of 3-(4,5-dimethylthiazol-2-yl)-2,5-diphenyltetrazolium bromide) tetrazolium (MTT) diluted in DMEM (1:10 v/v; MTT initial concentration 5 mg/mL) were added. After 4 h incubation, formazan crystals were solubilized with 0.1 mL of dimethylsulfoxide (DMSO), and the absorbance measured at 570 nm in a Microplate Reader (MultiSkan 60, Thermo Scientific; Spain). The relative cell viability (%) was calculated following Eq. (3).

$$\text{Cell viability}(\%) = (\text{Absorbance treated cells/Absorbance untreated control cells}) \times 100 \quad (3)$$

2.10. Interaction of protamine nanocapsules with cancer cells

The ability of isolated Pr NCs to get internalized by cancer cells and deliver the associated drugs (miRNA mimics and curcumin) was determined by confocal microscopy (Leica TCS SP5, Leica Microsystems, GmbH). Fuorescent nanocapsules, prepared with TAMRA-labeled protamine [41] or loaded with Cy5-RNA, were incubated for 4 h at 37 °C with SW480 cells (6.5×10^4 cells were seeded onto 12 mm diameter glass coverslips in a 24-well plate, 24 h before the experiment). Cells were then fixed with PFA 4% (w/v), permeabilized with Triton-X 100 0.2% (v/v), and counterstained with DAPI. Studies with Cy5-RNA-loaded Pr NCs were also performed by Fluorescence-Activated Cell Sorting (FACScan flow cytometer, BD biosciences). In this case, after 4 h incubation, cells were washed, trypsinized, and resuspended in 0.3 mL of PBS/FBS 2% (v/v) (approx. 1×10^6 cells/mL) prior to analysis.

Transfection experiments were performed in SW480 cells seeded in 6-well plates (2.5 × 105 cells/well), 24 h before the experiment. Cells were incubated for 4 h with miR-145- or miRNA-scr-loaded Pr NCs (5 μg of RNA/well), or curcumin-loaded Pr NCs (2.8 or 4.5 μg of curcumin/well) in a final volume of 1 mL of cell culture medium. Treatments were then removed, and cells continue growing in normal conditions up to 96 h. At 96 h, treatment effects were evaluated by means of RT-PCR, and western blot as described next.

Table 1
Physicochemical properties of protamine nanocapsules formulated with different PEG-based surfactants: PEG-stearate (PEG-st), D-α-tocopheryl polyethyleneglycol 1000 succinate (TPGS), and Tween® 80 (T80) (n = 3 ± SD).

Surfactant	Size (nm)	PDI[a]	Zeta potential (mV)	Reaction yield (%)
PEG-st	248 ± 17	0.1	+31 ± 11	83 ± 15
TPGS	191 ± 7	0.2	+23 ± 04	69 ± 21
T80	206 ± 17	0.1	+38 ± 02	78 ± 11

[a] PDI: polydispersity index.

2.11. Quantitative real-time PCR assay

For quantitative RT-PCR (Stratagene Mx 3000, Agilent Technologies), total miRNA was extracted from treated SW480 cells (MicroRNA Purification kit, Norgen Biotek Corporation). miRNA concentration and purity were determined with UV spectrophotometry (Nanodrop, Spectrophotometer ND-1000, Thermo Scientific). cDNA synthesis was carried out from 120 ng of total miRNA with the qSript™microRNA cDNA synthesis kit (Quanta Bioscience). Quantitative real-time PCR was carried out using PerfeCta® MicroRNA Assays (Quanta Biosciences), with a primer for miR-145 (has-miRNA-145-5p, 5′GUCCAGUUUUCCCAGGAAUCCCU3′, IDT). Small nuclear RNA, RNU6, was used as internal control for miRNA expression (5′CTCGCT TCGGCAGCACA3′; 5′AACGCTTCACGAATTTGCGT 3′). Each PCR cycle consisted of 2 min activation at 95 °C, 5 sec denaturation at 95 °C and 30 sec annealing at 60 °C (40 cycles). Quantitative data were analyzed by using the MxPro software (Agilent Technologies). Relative expression levels of miR-145 in each treatment group were calculated by the delta Ct method, as described by Livak et al. [42] in relation to RNU6 levels and normalized with respect to untreated control cells.

2.12. Western blot assay

Cells were harvested and homogenized in RIPA lysis buffer. Samples were centrifuged at 13,000 rpm for 20 min at 4 °C, and the supernatants collected for protein quantification by the Bradford assay. A total amount of 10 μg of protein lysate was separated using SDS-PAGE separation gels (4% stacking gel and 10% resolving gel), and electroblotted onto a nitrocellulose membrane (PerkinElmer Life Sciences, Inc., Boston, MA, USA). Non-specific binding sites were blocked for 1 h with 5% non-fat milk (w/v) in TTBS (TBS 20X with 1% (v/v) of Tween® 20). The membrane was then incubated overnight at 4 °C with antibodies for Akt, phospho-Akt (Ser473), p44/42 MAPK (ERK 1/2), phospo-p44/42 MAPK (ERK 1/2) (Thr202/Tyr204), IGF-1 Receptor β antibody (IGF-1R) and actin (Cell Signaling Technology®, Leiden, The Netherlands), diluted in TTBS with 5% of BSA following manufacturer recommendations. The membrane was then washed three times with TTBS for 10 min, and further incubated for 1 h with the secondary antibody (anti-rabbit or anti-mouse, Cell Signaling Technology®) at room temperature. The membrane was washed again three times with TTBS. Finally, immunoblots were developed with Pierce ECL (Enhanced chemoluminescence) Western blotting substrate (Thermo Scientific). The

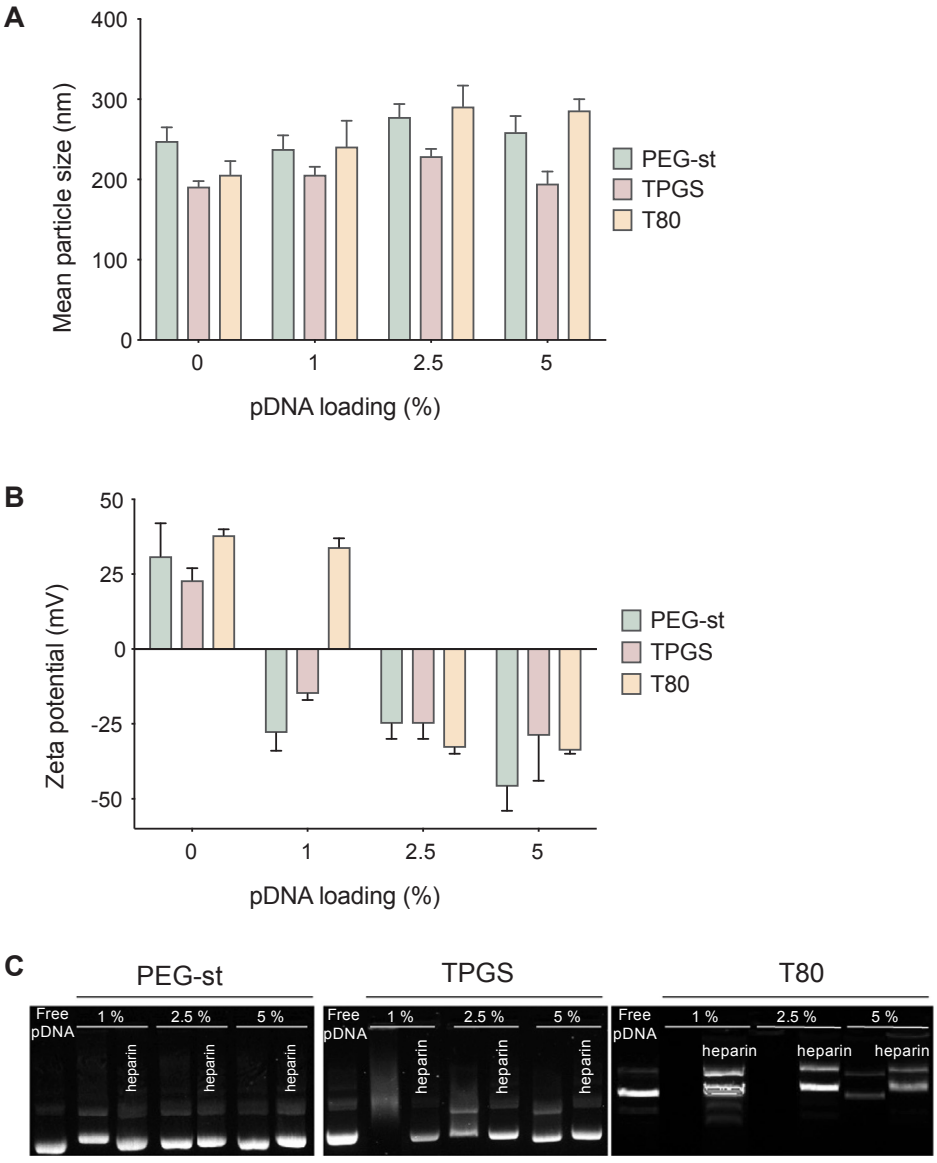

Fig. 1. Characterization of pDNA-loaded protamine nanocapsules formulated with different PEG-based surfactants: PEG-stearate (PEG-st), D-α-tocopheryl polyethyleneglycol 1000 succinate (TPGS), Tween® 80 (T80), and loaded with increasing amounts of pDNA (1%, 2.5% and 5% w/w). (A) Size. (B) Zeta potential. (C) Agarose gel electrophoresis; 1 μg of pDNA (either in its free form or associated to protamine nanocapsules) was loaded into the gel. A displacement experiment upon incubation with a 25-fold excess of heparin allowed the migration of the associated pDNA.

membranes were developed in a CURIX 60 (Agfa®) at different exposition times.

2.13. Cell proliferation and cell migration assays

Cell proliferation was evaluated 96 h after the treatment of cells. To evaluate cell proliferation, cells were harvested and counted with the TC20TM Automated Cell Counter (BIO-RAD, Madrid, Spain). In the case of migration, a wound-healing assay was performed as previously described by Hergueta-Redondo et al. [43]. After treatment, artificial wounds were created on the confluent cell monolayer using 10–100 μL pipette tips, and the detached cells were washed twice with PBS. Cells were cultured at 37 °C and 5% CO_2 and wound closure was monitored and photographed at time points 0, 24 and 96 h under a microscope (Olympus IX70). The wound closure area was calculated by analyzing the microscopy images with the software ImageJ (1.48d; National Institutes of Health, Bethesda, MD, USA).

2.14. Statistical analysis

Differences were statistically evaluated by one-way ANOVA followed by Tukey's method. All statistical analysis was conducted using GraphPad Prism (Version 6.0 software). A p value < 0.05 was considered to be significant.

3. Results and discussion

3.1. Optimization of protamine nanocapsules for gene therapy applications

We propose here the use of protamine nanocapsules (Pr NCs) with the aim of increasing the intracellular levels of oncosuppressor miR-145 and mediate an antitumoral therapeutic effect. Pr NCs were prepared by solvent displacement [39], which allows the controlled formation of vitamin E nano-droplets, stabilized with surfactants, and coated with protamine. Although protamine has been widely reported for its used in gene delivery [44], to the best of our knowledge, its inclusion in core-shell nanostructures aimed for miRNA replacement therapies has not

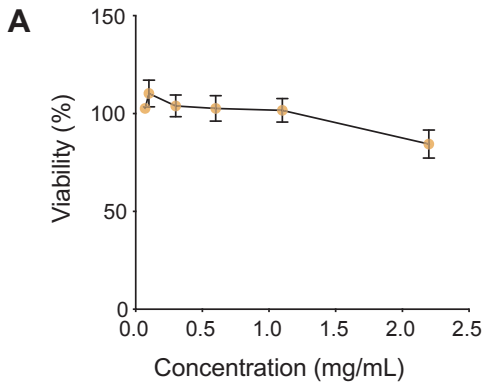

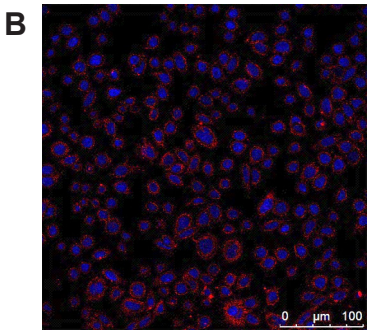

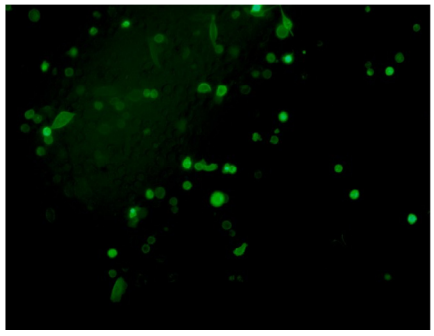

Fig. 2. Protamine nanocapsules (Pr NCs) interaction with SW480 cancer cells. (A) Cellular viability of SW480 cells after incubation with increased concentrations of Pr NCs (4 h incubation, at 37 °C, and up to 96 h growing in normal conditions; MTT assay). (B) Confocal image (maximum projection) of SW480 cells (cell nuclei staining with DAPI, blue channel), 4 h incubation with 5-TAMRA-labeled Pr NCs (red channel). (C) GFP expression after transfection of SW480 cells with pGFP-loaded Pr NCs, measured under the fluorescent microscope 96 h post-transfection (1 µg of pGFP per well, 4 h incubation). (For interpretation of the references to colour in this figure legend, the reader is referred to the web version of this article.)

been explored yet. Moreover, this unique structure also presents the advantage of allowing the encapsulation of lipophilic drugs within the oily core. Furthermore, the only work involving arginine-rich polymer NCs is the one describing the association of miRNA to polyarginine NCs [45]. Therefore, first experiments were conducted to optimize their composition and ensure an efficient association of the polynucleotides to the protamine shell. Bearing this in mind, we studied three different compositions, which differ in the type of PEGylates surfactants, i.e. PEG-st, TPGS, and Tween® 80, with variable length and density of PEG. Characterization of the resulting Pr NCs (Table 1), revealed a small nanoparticle size in all cases (< 250 nm), a low polydispersity index (0.2), a cationic surface charge (zeta potential ≥ +23 mV), and a yield of production around 69–83%. Despite Pr NCs were similar regarding these parameters, irrespective of the type of surfactants, important differences were observed with respect to their capacity to condense polynucleotides (Fig. 1).

In a first screening, and based on previous experience by our group [46–49] Pr NCs were loaded with increasing amounts of pDNA encoding a green fluorescent protein (pGFP). As observed, a slight increase in size (Fig. 1A), and an inversion in the zeta potential values (Fig. 1B), were observed in most cases after the plasmid association. However, only Pr NCs prepared with Tween® 80, the surfactant with the shortest PEG chain and a branched structure, could efficiently associate the plasmid (Fig. 1C). This is in line with previous reported results, which evidenced that surfactants with shorter PEO chains, such as Tween® 80, are less prone to interfere with the association of polypeptides to nanocapsules [32]. For this reason, the formulation of Pr NCs prepared with Tween® 80 was the one selected for further studies.

Next experiments were aimed to determine the ability of Pr NCs to interact with colorectal cancer cells. Cell viability studies indicate that SW480 cells are viable after exposition to concentrations up to 2.2 mg/mL (Fig. 2A). These results are particularly good considering that Pr NCs are cationic nanosystems, which are typically more toxic than neutral and anionic carriers [50]. Moreover, our results are in line with previously reported cytotoxicity data of Pr NCs in Caco-2 cells [51] and also protamine-based liposomes in breast cancer and embryonic kidney cells [18,35]. In addition, cell internalization studies performed with TAMRA-labeled Pr NCs (prepared by conjugation of 5-TAMRA to protamine following a previously reported protocol [41]), show an efficient uptake and homogeneous distribution of the fluorescence around the cell nuclei (Fig. 2B). Importantly, transfection experiments proved that Pr NCs could efficiently transfect colorectal cancer cells (Fig. 2C). Apart from the known role of protamine for mediating efficient gene transfer to cancer cells [18,34–38], the incorporation of Tween® 80 into the formulation could also have additional advantages for gene therapy applications, favoring their uptake [52].

3.2. Development and evaluation of miR-145-loaded protamine nanocapsules

Association of miR-145 mimics to Pr NCs was subsequently pursued for a theoretical loading of 1.5% (w/w) (0,54 mg/mL). miR-145-loaded Pr NCs had a similar size to the one of the unloaded nanocapsules (Fig. 3A). However, a decrease in the zeta potential values, indicative of the efficient association of the nucleic acids, was observed. This association was also confirmed by a gel retardation assay followed by heparin displacement (Fig. 3B and C). Confocal fluorescence microscopy studies showed that Pr NCs could efficiently deliver the associated miRNAs to the cell cytoplasm of colorectal cancer cells (Fig. 3D, the red signal corresponding to Cy5-labelled RNA, and the blue signal to the cell nuclei stained with DAPI). This improved internalization, confirmed by FACS (Fig. 3E), resulted into a 33-fold increase of the intracellular miR-145 levels for transfected cells, with respect to cells transfected with the scrambled sequence (Fig. 3F). These results are really promising, being far superior to those recently reported after (i) transfection of HepG2 cells with a plasmidic form of miR-145 associated to cationic liposomes (9-fold increase) [18], (ii) transfection of HTC-116 cells with a plasmidic form of miR-145 associated to PLGA/PEI/HA complexes (11-fold increase) [19], and transfection of colorectal cancer SW6290 cells with miR-145 mimics associated to a

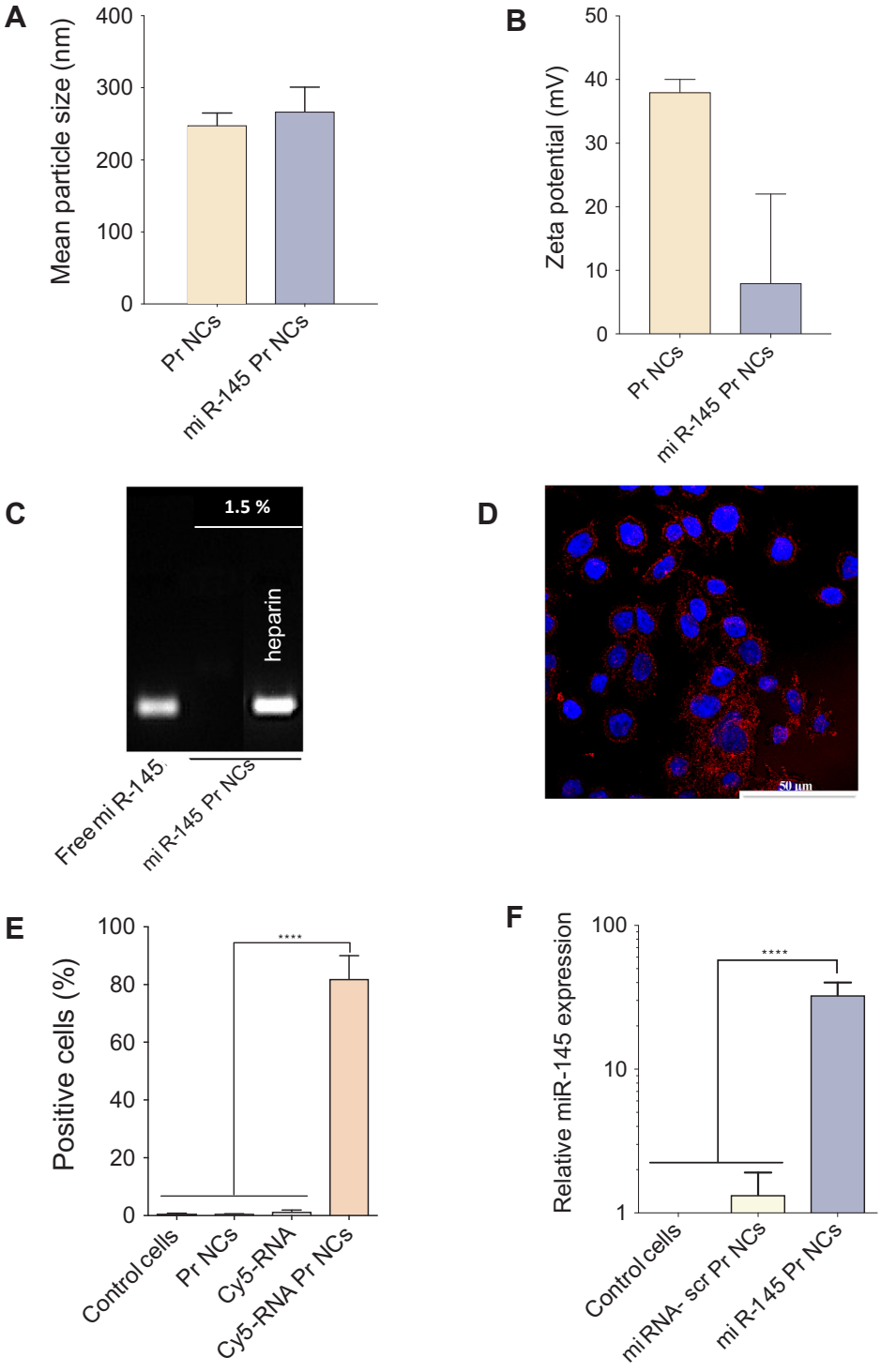

Fig. 3. Characterization of miR-145-loaded protamine nanocapsules (miR-145 Pr NCs). (A) Size and (B) Zeta potential of miR-145 Pr NCs, compared to unloaded nanocapsules (Pr NCs). (C) The efficiency of the miRNA association was determined by agarose gel electrophoresis; (Lane 1: 1 µg of free miRNA; Lane 2: 1 µg of miRNA loaded into Pr NCs; Lane 3: 1 µg of miRNA loaded into Pr NCs and displaced with a 25-fold excess of heparin (w/w)). (D) SW480 colorectal cancer cells after incubation with Cy5-RNA-loaded Pr NCs (Cy5-RNA: red channel. Cell nuclei (DAPI): Blue channel). (E) Percentage of Cy5-RNA positive SW480 cells determined by FACS, after incubation with unloaded Pr NCs, Cy5-RNA in solution, or Cy5-RNA loaded Pr NCs (Cy5-RNA Pr NCs). (F) Relative expression of miR-145 in SW480 cells after transfection with Pr NCs loaded with a scrambled sequence (miRNA-scr Pr NCs) or with miR-145 (miR-145 Pr NCs) (data normalized against RNU6). (n = 3 ± SD). (For interpretation of the references to colour in this figure legend, the reader is referred to the web version of this article.)

lentiviral vector (8.2-fold increase) [53]. As mentioned before, the excellent internalization properties mediated by Pr NCs can be related to the fact that protamine is a cell penetrating peptide that can promote cellular membrane translocation and to the membrane permeabilization properties of Tween® 80 [52].

3.3. Optimization of protamine nanocapsules for miRNA delivery following a layer-by-layer approach

A further optimization, consisting in the addition of an external layer of protamine to the formulation, was carried out with the purpose of improving the interaction and intracellular delivery of miR-145-loaded Pr NCs to colorectal cancer cells. It is well known that protamine can mediate a strong interaction with cancer cells, and the presence of a second protamine layer, on top of the miRNA layer, could also protect it from degradation [45,54]. Similar approaches have recently been reported for sulfate dextran-chitosan and polyarginine-hyaluronic acid nanocapsules formulated for antigen delivery, and co-delivery of a RNAi and chemokine, respectively [45,55]. The resulting *sandwich-like* structure (Fig. 4A), protamine-coated miR-145 Pr NCs (Pr miR-145 Pr NCs) had similar physicochemical properties to the uncoated formulations (301 ± 24 nm in size with a low polydispersity index of 0.1 and a

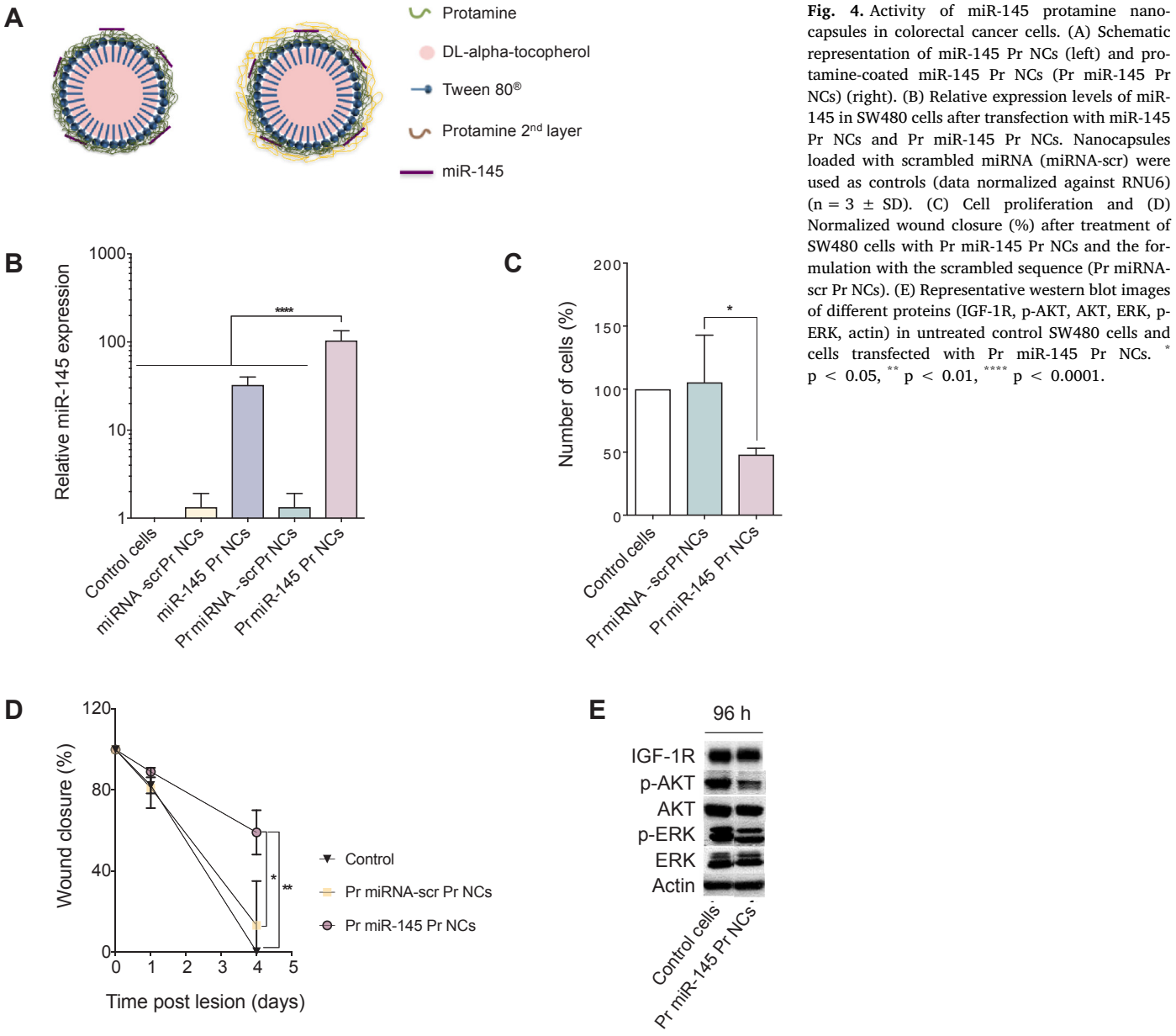

Fig. 4. Activity of miR-145 protamine nanocapsules in colorectal cancer cells. (A) Schematic representation of miR-145 Pr NCs (left) and protamine-coated miR-145 Pr NCs (Pr miR-145 Pr NCs) (right). (B) Relative expression levels of miR-145 in SW480 cells after transfection with miR-145 Pr NCs and Pr miR-145 Pr NCs. Nanocapsules loaded with scrambled miRNA (miRNA-scr) were used as controls (data normalized against RNU6) (n = 3 ± SD). (C) Cell proliferation and (D) Normalized wound closure (%) after treatment of SW480 cells with Pr miR-145 Pr NCs and the formulation with the scrambled sequence (Pr miRNA-scr Pr NCs). (E) Representative western blot images of different proteins (IGF-1R, p-AKT, AKT, ERK, p-ERK, actin) in untreated control SW480 cells and cells transfected with Pr miR-145 Pr NCs. * $p < 0.05$, ** $p < 0.01$, **** $p < 0.0001$.

Table 2
Physicochemical properties of protamine nanocapsules loaded with curcumin (n = 3 ± SD).

Curcumin (w/w, %)[a]	Size (nm)	PDI[b]	Zeta potential (mV)	EE (%)[c]	Curcumin (μg/mL)
–	206 ± 17	0.1	+38 ± 2	–	–
0.75	228 ± 18	0.1	+34 ± 6	90 ± 6	90.5
2.2	248 ± 29	0.2	+30 ± 5	64 ± 6	188.7

[a] % of curcumin loading (w/w) with respect to the total mass of nanocapsules.
[b] PDI: polydispersity index.
[c] EE: curcumin encapsulation efficiency.

zeta potential of +12 ± 8 mV). An agarose gel electrophoresis was subsequently run to confirm that miRNA was not displaced by the addition of the outer layer of protamine to the formulation (data not shown). With respect to the transfection efficiency, although all formulations were able to efficiently increase the intracellular levels of miR-145, the additional coating of miR-145 Pr NCs with protamine led to significantly higher transfection values, almost three times higher than the increase observed for the uncoated miRNA-145 Pr NCs (33-fold increase) (Fig. 4B). This increase in the intracellular levels of oncosuppressor miR-145 efficiently translated into a strong inhibition of the ability of the transfected SW480 cells to proliferate and migrate (Fig. 4C and D). On view of the ability of Pr miR-145 Pr NCs to reduce the phosphorylation of AKT and ERK (Fig. 4E), we were able to confirm that the delivered miR-145 lead to functional effects related to the regulation of the EGFR pathway, and activation of the RAS–RAF–MAP kinase and the PI3K–PTEN–Akt pathways, controlling cell proliferation and cell survival [56]. Despite of the described decrease of IGF-1R levels related to the increase on the intracellular levels of miR-145 in colorectal cells [57], in our case and at the tested conditions, this effect was not observed for Pr miR-145 Pr NCs.

3.4. Development and evaluation of curcumin-loaded protamine nanocapsules

As it was commented before, we also wanted to evaluate the potential of Pr NCs to mediate an increase in the intracellular levels of

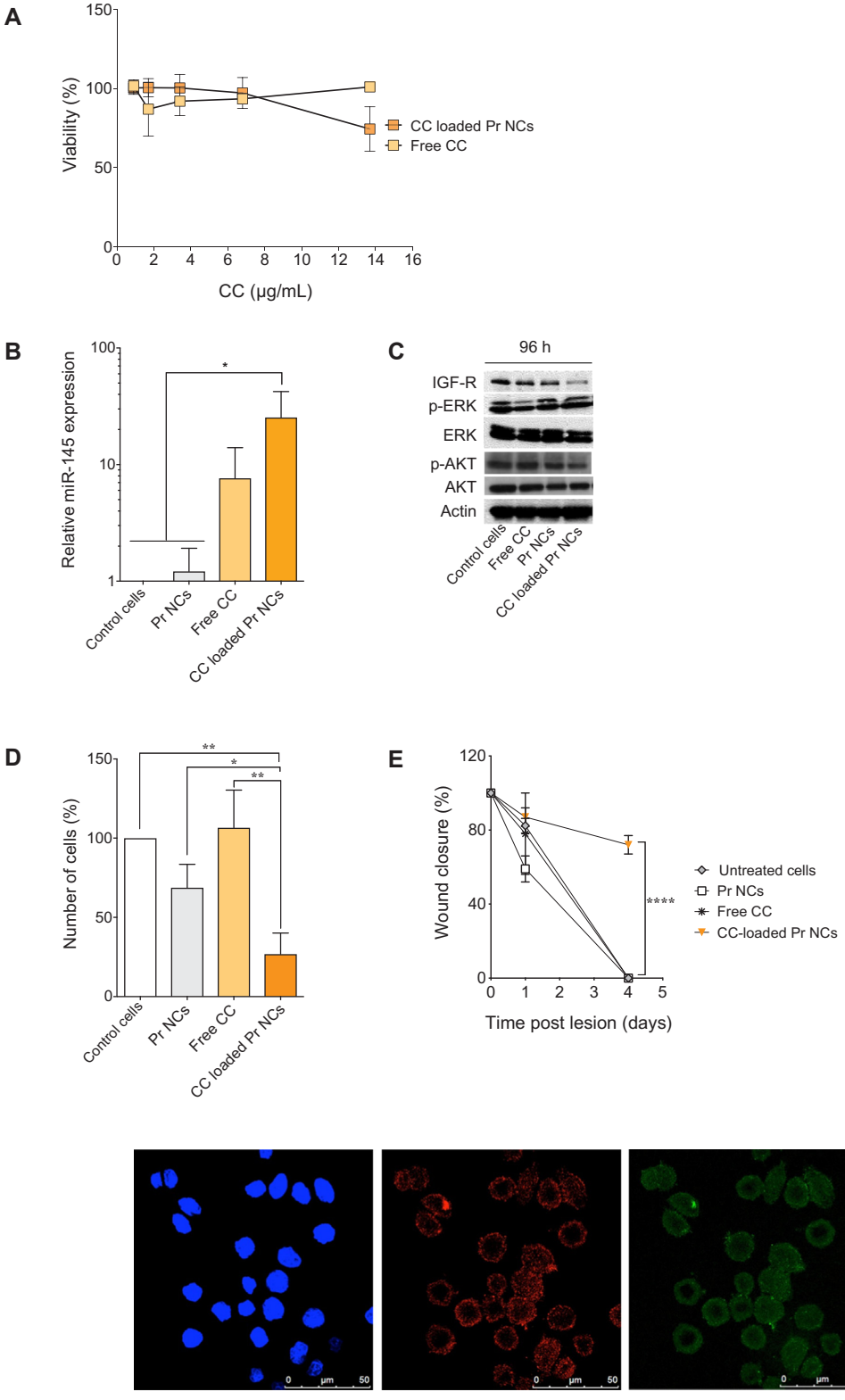

Fig. 5. Activity of curcumin-loaded protamine nanocapsules (CC loaded Pr NCs) in SW480 colorectal cancer cells. (A) MTT assay after treatment with curcumin-loaded protamine nanocapsules (CC-loaded Pr NCs) and curcumin in aqueous suspension (Free CC). (B) Relative expression levels of miR-145 (data normalized against RNU6) of cells treated with Pr NCs (no CC loaded), free CC, or CC-loaded Pr NCs (dose 2.8 µg curcumin/well). (C) Representative western blot images of IGF-1R, ERK, p-ERK, AKT, p-AKT, and actin proteins extracted after cell treatment with unloaded Pr NCs, free CC or CC-loaded Pr NCs (dose of 4.5 µg curcumin/well). * $p < 0.05$, ** $p < 0.01$; **** $p < 0.0001$. 4 h treatment; analysis was performed at 96 h post-treatment.

Fig. 6. Interaction of curcumin- and miR-145- loaded protamine nanocapsules with SW480 colorectal cancer cells. Confocal image of cells treated with curcumin- (green channel) and Cy5-miR- (red channel) loaded into Pr NCs. Cell nuclei (DAPI): Blue channel. Maximum Projections. (For interpretation of the references to colour in this figure legend, the reader is referred to the web version of this article.)

miR-145 and a therapeutic effect, following a different approach, i.e. by delivering the antitumoral drug curcumin, reported to act in several pathways related to miRNA modulation [8,9,58–60]. Due to its hydrophobic character, curcumin was loaded within the oily core of Pr NCs. Two different drug loadings were tested, 0.75 and 2.2% (w/w with respect to the total weight of components). As seen in Table 2, the physicochemical characterization shows curcumin-loaded Pr NCs with a small size below 250 nm, a narrow distribution, and a positive surface charge, irrespective of the drug content. Moreover, encapsulation efficiencies of 64–90%, depending on the initial theoretical drug loading,

were reported, similarly to those observed for other nanoparticle compositions, as for example soybean nanoparticles, PEG-PLGA nanoparticles, and CS/PEG/PLGA nanoparticles [30,31,61].

In vitro experiments proved that the encapsulated curcumin was successfully delivered to SW480 colorectal cancer cells. The cytotoxic effect of the curcumin-loaded Pr NCs was superior to the one of free curcumin (Fig. 5A). To study their capacity to increase the intracellular miR-145 levels, cells were treated at subtherapeutic doses of curcumin (i.e. without compromising the cell viability). Results confirmed that curcumin can indeed increase miR-145, especially when it is encapsulated within Pr NCs (Fig. 5B). Looking at proteins, although no differences were detected for the ERK/p-ERK and AKT/p-AKT levels in curcumin-loaded Pr NCs treated cells, compared to controls, there was a marked reduction in the levels of IGF-1R (Fig. 5C), in agreement with previous reports [27]. Moreover, we confirmed the potential of curcumin-loaded Pr NCs to mediate a reduction in cellular proliferation (Fig. 5D) and migration (Fig. 5E) compared to cells treated with free curcumin, empty Pr NCs, and the control untreated cells.

3.5. Potential of protamine nanocapsules for co-delivery of miR-145 mimics and curcumin

We finally attempted the co-encapsulation of both miR-145 and curcumin into Pr NCs for the development of a combination therapy, taking advantage of the core-shell disposition of the components that allow entrapment of hydrophobic molecules into the oily core and association of hydrophilic biomolecules onto the polymeric shell [62]. Considering that cancer resistance is a common phenomenon related to cancer progression, co-administration of several molecules into the same entity could help circumventing this problem. Two different combination therapies based on the combination of gene therapies and hydrophobic anticancer drugs into nanocapsules have been recently published showing promising results. One work relates to the application of cationic poly-lactide nanocapsules for the co-delivery of doxorubicin and interleukin-8 siRNA [63], and the other to lipid nanocapsules functionalized with poly(ethyleneimine) (PEI) moieties for co-delivery of pDNA and paclitaxel [64].

The association of both molecules into Pr NCs was successfully achieved, with theoretical loadings of 0.75% and 1.5% w/w for curcumin and miRNA respectively, rendering encapsulation efficiencies superior to 90% for both molecules. The size and zeta potential were similar to those reported for NCs that encapsulate a single agent (263 ± 23 nm, and -4 ± 2 mV). Additionally, confocal microscopy studies, showed a strong co-localization of fluorescent miRNA-Cy5 (red) and curcumin (green) into the cell cytoplasm (Fig. 6). This has allowed us confirming that both types of molecules could indeed be simultaneously delivered to colorectal cancer cells, opening a new perspective in the design of combinatory therapies for miRNA modulation in cancer cells. Given the activity of both molecules, miRNA mimics and curcumin, in modulating determinant biological processes in cancer progression, the proposed nanosystem could be a promising strategy to test their synergistic effect as a novel anticancer therapy. Further studies will be oriented in that direction.

4. Conclusion

In summary, we have successfully proved that Pr NCs can be specifically adapted for gene replacement therapies to restore the intracellular levels of oncosuppressor miRNAs with therapeutic purposes. We have shown the potential of our formulation to encapsulate miR-145 mimics and curcumin, alone or in combination, and proved that the developed formulations can hamper tumor proliferation and migration in colorectal cancer cells.

5. Summary points

- Protamine nanocapsules with a nanometric size and positive zeta potential were conveniently adapted to allow an efficient association of miRNA mimics, curcumin, and the combination of both.
- Protamine nanocapsules show a very efficient internalization by colorectal cancer cells.
- Protamine nanocapsules successfully deliver miRNA mimics and curcumin to colorectal cancer cells, leading to an increase in the intracellular levels of oncosuppressor miR-145.
- Cancer cells treated with miR-145 mimics and curcumin-loaded protamine nanocapsules show a decrease in their proliferation rate and migration capacity, related to an increase in oncosuppresor miR-145.

Author contributions

The manuscript was written through contributions of all authors. All authors have given approval to the final version of the manuscript.

Acknowledgements

The authors acknowledge Prof. Anxo Vidal for his contribution to FACs analysis, Cristina Mondelo, who assisted with the preparation of the nanocapsules, and Carmen Abuín, for the technical support. This work was supported by Carlos III Health Institute/FEDER funds (CP12/03150 and PI15/00828), by Xunta de Galicia/FEDER funds (10PXIB203064R and GRC2013-043), and by the Fundación Científica de la Asociación Española Contra el Cáncer (AECC), Spain.

References

[1] V. Aran, A.P. Victorino, L.C. Thuler, C.G. Ferreira, Colorectal cancer: epidemiology, disease mechanisms and interventions to reduce onset and mortality, Clin. Colorectal Can. 15 (2016) 195–203, https://doi.org/10.1016/j.clcc.2016.02.008.
[2] M. Arnold, M.S. Sierra, M. Laversanne, I. Soerjomataram, A. Jemal, F. Bray, Global patterns and trends in colorectal cancer incidence and mortality, Gut. (2016) gutjnl-2015-310912. doi: 10.1136/gutjnl-2015-310912.
[3] W. Ji, B. Sun, C. Su, Targeting microRNAs in cancer gene therapy, Genes (Basel) 8 (2017), https://doi.org/10.3390/genes8010021.
[4] B. Zeshan, A. Sadaf, N.H. Othman, Recent progress in delivery of cancer related microRNAs, J. Nanosci. Nanotechnol. 16 (2016) 6622–6633, https://doi.org/10.1166/jnn.2016.11360.
[5] R. Gambari, E. Brognara, D. Spandidos, E. Fabbri, Targeting oncomiRNAs and mimicking tumor suppressor miRNAs: new trends in the development of miRNA therapeutic strategies in oncology (Review), Int. J. Oncol. (2016) 1–28, https://doi.org/10.3892/ijo.2016.3503.
[6] R. Rupaimoole, F.J. Slack, MicroRNA therapeutics: towards a new era for the management of cancer and other diseases, Nat. Rev. Drug Discov. 16 (2017) 203–222, https://doi.org/10.1038/nrd.2016.246.
[7] M.L. Abba, N. Patil, J.H. Leupold, M. Moniuszko, J. Utikal, J. Niklinski, H. Allgayer, MicroRNAs as novel targets and tools in cancer therapy, Cancer Lett. 387 (2017) 84–94, https://doi.org/10.1016/j.canlet.2016.03.043.
[8] Y. Li, F. Sarkar, Targeting microRNAs: molecular basis of cancer prevention, Mol. Targets Strateg. Can. Prev. (2016) 61–84, https://doi.org/10.1007/978-3-319-31254-5.
[9] B. Biersack, Current state of phenolic and terpenoidal dietary factors and natural products as non-coding RNA/microRNA modulators for improved cancer therapy and prevention, Non-Coding RNA Res (2016) 1–23, https://doi.org/10.1016/j.ncrna.2016.07.001.
[10] C. Wang, W. Tao, S. Ni, Q. Chen, Z. Zhao, L. Ma, Y. Fu, Z. Jiao, Tumor-suppressive microRNA-145 induces growth arrest by targeting SENP1 in human prostate cancer cells, Can. Sci. 106 (2015) 375–382, https://doi.org/10.1111/cas.12626.
[11] W. Wang, G. Ji, X. Xiao, X. Chen, W.-W. Qin, F. Yang, Y.-F. Li, L.-N. Fan, W.-J. Xi, Y. Huo, W.-H. Wen, A.-G. Yang, T. Wang, Epigenetically regulated miR-145 suppresses colon cancer invasion and metastasis by targeting LASP1, Oncotarget. 7 (2016) 68674–68687, https://doi.org/10.18632/oncotarget.11919.
[12] Y. Yu, P. Nangia-Makker, L. Farhana, S.G. Rajendra, E. Levi, A.P.N. Majumdar, miR-21 and miR-145 cooperation in regulation of colon cancer stem cells, Mol. Can. 14 (2015) 1–10, https://doi.org/10.1186/s12943-015-0372-7.
[13] H. Zhao, X. Kang, X. Xia, L. Wo, X. Gu, Y. Hu, X. Xie, H. Chang, L. Lou, X. Shen, miR-145 suppresses breast cancer cell migration by targeting FSCN-1 and inhibiting epithelial-mesenchymal transition, Am. J. Transl. Res. 8 (2016) 3106–3114.
[14] R. Matsushita, H. Yoshino, H. Enokida, Y. Goto, K. Miyamoto, M. Yonemori, S. Inoguchi, M. Nakagawa, N. Seki, Regulation of UHRF1 by dual-strand tumor-suppressor microRNA-145 (miR-145-5p and miR-145-3p): Inhibition of bladder

cancer cell aggressiveness, Oncotarget. 7 (2016) 1–28, https://doi.org/10.18632/oncotarget.8668.
[15] A. Ganju, S. Khan, B.B. Hafeez, S.W. Behrman, M.M. Yallapu, S.C. Chauhan, M. Jaggi, miRNA nanotherapeutics for cancer, Drug Discov. Today 22 (2017) 424–432, https://doi.org/10.1016/j.drudis.2016.10.014.
[16] S. Setua, S. Khan, M.M. Yallapu, S.W. Behrman, M. Sikander, S.S. Khan, M. Jaggi, S.C. Chauhan, Restitution of tumor suppressor microRNA-145 using magnetic nanoformulation for pancreatic cancer therapy, J. Gastrointest. Surg. 21 (2017) 94–105, https://doi.org/10.1007/s11605-016-3222-z.
[17] A.F. Ibrahim, U. Weirauch, M. Thomas, A. Grünweller, R.K. Hartmann, A. Aigner, MicroRNA replacement therapy for miR-145 and miR-33a is efficacious in a model of colon carcinoma, Ther. Targets, Chem. Biol. 71 (2011) 5214–5224, https://doi.org/10.1158/0008-5472.CAN-10-4645.
[18] J. Tao, W.-F. Ding, X.-H. Che, Y.-C. Chen, F. Chen, X.-D. Chen, X.-L. Ye, S.-B. Xiong, Optimization of a cationic liposome-based gene delivery system for the application of miR-145 in anticancer therapeutics, Int. J. Mol. Med. 37 (2016) 1345–1354, https://doi.org/10.3892/ijmm.2016.2530.
[19] G. Liang, Y. Zhu, A. Jing, J. Wang, F. Hu, W. Feng, Z. Xiao, B. Chen, Cationic microRNA-delivering nanocarriers for efficient treatment of colon carcinoma in xenograft model, Gene Ther. (2016) 1–10, https://doi.org/10.1038/gt.2016.60.
[20] G. Chiou, J. Cherng, H. Hsu, M. Wang, C. Tsai, K.-H. Lu, Y. Chien, S.-C. Hung, Y.-W. Chen, C.-I. Wong, L.-M. Tseng, P.-I. Huang, C.-C. Yu, W.-H. Hsu, S.-H. Chiou, Cationic polyurethanes-short branch PEI-mediated delivery of Mir145 inhibited epithelial – mesenchymal transdifferentiation and cancer stem-like properties and in lung adenocarcinoma, J. Control. Release. 159 (2012) 240–250, https://doi.org/10.1016/j.jconrel.2012.01.014.
[21] M.A. Alam, F.I. Al-Jenoobi, A.M. Al-Mohizea, Everted gut sac model as a tool in pharmaceutical research: limitations and applications, J. Pharm. Pharmacol. 64 (2012) 326–336, https://doi.org/10.1111/j.2042-7158.2011.01391.x.
[22] D. Pramanik, N.R. Campbell, C. Karikari, R. Chivukula, O.A. Kent, J.T. Mendell, A. Maitra, Restitution of tumor suppressor microRNAs using a systemic nanovector inhibits pancreatic cancer growth in mice, Mol. Can. Ther. 10 (8) (2011) 1470–1480, https://doi.org/10.1158/1535-7163.MCT-11-0152.
[23] Y. Panahi, Y. Ahmadi, M. Teymouri, T.P. Johnston, A. Sahebkar, Curcumin as a potential candidate for treating hyperlipidemia: a review of cellular and metabolic mechanisms, J. Cell. Physiol. 233 (2018) 141–152, https://doi.org/10.1002/jcp.25756.
[24] A.B. Kunnumakkara, D. Bordoloi, C. Harsha, K. Banik, S.C. Gupta, B.B. Aggarwal, Curcumin mediates anticancer effects by modulating multiple cell signaling pathways, Clin. Sci. 131 (2017) 1781–1799, https://doi.org/10.1042/CS20160935.
[25] A. Allegra, V. Innao, S. Russo, D. Gerace, A. Alonci, C. Musolino, Anticancer activity of curcumin and its analogues: preclinical and clinical studies, Cancer Invest. 1–22 (2016).
[26] A.B. Kunnumakkara, D. Bordoloi, G. Padmavathi, J. Monisha, N.K. Roy, S. Prasad, B.B. Aggarwal, Curcumin, the golden nutraceutical: multitargeting for multiple chronic diseases, Br. J. Pharmacol. 174 (2017) 1325–1348, https://doi.org/10.1111/bph.13621.
[27] V.P. Brahmkhatri, C. Prasanna, H.S. Atreya, Insulin-like growth factor system in cancer: novel targeted therapies, Biomed Res. Int. 2015 (2015) 1–24.
[28] P. Anand, A.B. Kunnumakkara, R.A. Newman, B.B. Aggarwal, Bioavailability of curcumin: problems and promises, Mol. Pharm. 4 (2007) 807–818, https://doi.org/10.1021/mp700113r.
[29] M.T. Mirgani, B. Isacchi, M. Sadeghizadeh, F. Marra, A.R. Bilia, S.J. Mowla, F. Najafi, E. Babaei, Dendrosomal curcumin nanoformulation downregulates pluripotency genes via miR-145 activation in U87MG glioblastoma cells, Int. J. Nanomed. 9 (2014) 403–417, https://doi.org/10.2147/IJN.S48136.
[30] D. Duan, A. Wang, L. Ni, L. Zhang, X. Yan, Y. Jiang, H. Mu, Z. Wu, K. Sun, Y. Li, Trastuzumab- and Fab' fragment-modified curcumin PEG-PLGA nanoparticles: preparation and evaluation in vitro and in vivo, Int. J. Nanomed. 13 (2018) 1831–1840, https://doi.org/10.2147/IJN.S153795.
[31] G. Arya, M. Das, S.K. Sahoo, Evaluation of curcumin loaded chitosan/PEG blended PLGA nanoparticles for effective treatment of pancreatic cancer, Biomed. Pharmacother. 102 (2018) 555–566, https://doi.org/10.1016/j.biopha.2018.03.101.
[32] J.V. González-Aramundiz, E. Presas, I. Dalmau-Mena, S. Martínez-Pulgarín, C. Alonso, J.M. Escribano, M.J. Alonso, N.S. Csaba, Rational design of protamine nanocapsules as antigen delivery carriers, J. Control. Release. 245 (2017) 62–69, https://doi.org/10.1016/j.jconrel.2016.11.012.
[33] J.V. González-Aramundiz, M. Peleteiro, Á. González-Fernández, M.J. Alonso, N.S. Csaba, Protamine nanocapsules for the development of thermostable adjuvanted nanovaccines, Mol. Pharm. 15 (2018) 5653–5664, https://doi.org/10.1021/acs.molpharmaceut.8b00852.
[34] D. Delgado, A. del Pozo-Rodríguez, M.Á. Solinís, M. Avilés-Triqueros, B.H.F. Weber, E. Fernández, A.R. Gascón, Dextran and protamine-based solid lipid nanoparticles as potential vectors for the treatment of X-linked juvenile retinoschisis, Hum. Gene Ther. 23 (2012) 345–355, https://doi.org/10.1089/hum.2011.115.
[35] S. Wang, M. Cao, X. Deng, X. Xiao, Z. Yin, Q. Hu, Z. Zhou, F. Zhang, R. Zhang, Y. Wu, W. Sheng, Y. Zeng, Degradable hyaluronic acid/protamine sulfate interpolyelectrolyte complexes as miRNA-delivery nanocapsules for triple-negative breast cancer therapy, Adv. Healthc. Mater. 4 (2015) 281–290, https://doi.org/10.1002/adhm.201400222.
[36] M. Liu, B. Feng, Y. Shi, C. Su, H. Song, W. Cheng, L. Zhao, Protamine nanoparticles for improving shRNA-mediated anti-cancer effects, Nanoscale Res. Lett. 10 (2015), https://doi.org/10.1186/s11671-015-0845-z.
[37] F. Erdem-Çakmak, S. Özbaş-Turan, E. Şalva, J. Akbuğa, Comparison of VEGF gene silencing efficiencies of chitosan and protamine complexes containing shRNA, Cell Biol. Int. 38 (2014) 1260–1270, https://doi.org/10.1002/cbin.10317.
[38] K. Kanda, Y. Kodama, T. Kurosaki, M. Imamura, H. Nakagawa, T. Muro, N. Higuchi, T. Nakamura, T. Kitahara, M. Honda, H. Sasaki, Ternary complex of plasmid DNA with protamine and γ-polyglutamic acid for biocompatible gene delivery system, Biol. Pharm. Bull. 36 (2013) 1794–1799, https://doi.org/10.1248/bpb.b13-00479.
[39] M.V. Lozano, G. Lollo, M. Alonso-Nocelo, J. Brea, a. Vidal, D. Torres, M.J. Alonso, Polyarginine nanocapsules: a new platform for intracellular drug delivery, J. Nanoparticle Res 15 (2013), https://doi.org/10.1007/s11051-013-1515-7.
[40] A. Beloqui, P.B. Memvanga, R. Coco, S. Reimondez-Troitiño, M. Alhouayek, G.G. Muccioli, M.J. Alonso, N. Csaba, M. de la Fuente, V. Préat, A comparative study of curcumin-loaded lipid-based nanocarriers in the treatment of inflammatory bowel disease, Colloids Surfaces B Biointerfaces 143 (2016) 327–335, https://doi.org/10.1016/j.colsurffb.2016-03.038.
[41] S. Reimondez-Troitiño, I. Alcalde, N. Csaba, A. Íñigo-Portugués, M. de la Fuente, F. Bech, A.C. Riestra, J. Merayo-Lloves, M.J. Alonso, Polymeric nanocapsules: a potential new therapy for corneal wound healing, Drug Deliv. Transl. Res. 6 (2016) 708–721, https://doi.org/10.1007/s13346-016-0312-0.
[42] K.J. Livak, T.D. Schmittgen, Analysis of relative gene expression data using real-time quantitative PCR and the 2 CT method, Methods. 25 (2001) 402–408. doi: 10.1006/meth.2001.1262.
[43] M. Hergueta-Redondo, D. Sarrió, Á. Molina-Crespo, D. Megias, A. Mota, A. Rojo-Sebastian, P. García-Sanz, S. Morales, S. Abril, A. Cano, H. Peinado, G. Moreno-Bueno, Gasdermin-B promotes invasion and metastasis in breast cancer cells, PLoS ONE 9 (2014) 1–15, https://doi.org/10.1371/journal.pone.0090099.
[44] J.V. González-Aramundiz, M.V. Lozano, A. Sousa-Herves, E. Fernandez-Megia, N. Csaba, Polypeptides and polyaminoacids in drug delivery, Expert Opin. Drug Deliv. 9 (2012) 183–201, https://doi.org/10.1517/17425247.2012.647906.
[45] A.M. Ledo, M.S. Sasso, V. Bronte, I. Marigo, B.J. Boyd, M. García-Fuentes, M.J. Alonso, Co-delivery of RNAi and chemokine by polyarginine nanocapsules enables the modulation of myeloid-derived suppressor cells, J. Control. Release. 295 (2019) 60–73, https://doi.org/10.1016/j.jconrel.2018.12.041.
[46] N. Csaba, P. Caamaño, A. Sánchez, F. Domínguez, M.J. Alonso, PLGA:poloxamer and PLGA:poloxamine blend nanoparticles: new carriers for gene delivery, Biomacromolecules 6 (2005) 271–278, https://doi.org/10.1021/bm049577p.
[47] N. Csaba, M. Köping-Höggård, M.J. Alonso, Ionically crosslinked chitosan/tripolyphosphate nanoparticles for oligonucleotide and plasmid DNA delivery, Int. J. Pharm. 382 (2009) 205–214, https://doi.org/10.1016/j.ijpharm.2009.07.028.
[48] M de la Fuente, B Seijo, M J Alonso, Design of novel polysaccharidic nanostructures for gene delivery, Nanotechnology 19 (7) (2008) 075105, https://doi.org/10.1088/0957-4484/19/7/075105.
[49] M. Hornof, M. de la Fuente, M. Hallikainen, R.H. Tammi, A. Urtti, Low molecular weight hyaluronan shielding of DNA/PEI polyplexes facilitates CD44 receptor mediated uptake in human corneal epithelial cells, J. Gene Med. 10 (2008) 70–80, https://doi.org/10.1002/jgm.
[50] A. Sukhanova, S. Bozrova, P. Sokolov, M. Berestovoy, A. Karaulov, I. Nabiev, Dependence of Nanoparticle Toxicity on Their Physical and Chemical Properties (2018), https://doi.org/10.1186/s11671-018-2457-x.
[51] L.N. Thwala, A. Beloqui, N.S. Csaba, D. González-Touceda, S. Tovar, C. Dieguez, M.J. Alonso, V. Préat, The interaction of protamine nanocapsules with the intestinal epithelium: a mechanistic approach, J. Control. Release. 243 (2016) 109–120, https://doi.org/10.1016/j.jconrel.2016.10.002.
[52] A.A. Doolaanea, N. 'Izzati Mansor, N.H. Mohd Nor, F. Mohamed, Cellular uptake of Nigella sativa oil-PLGA microparticle by PC-12 cell line, J. Microencapsul. 31 (2014) 600–608, https://doi.org/10.3109/02652048.2014.898709.
[53] C. Li, N. Xu, Y.Q. Li, Y. Wang, Z.T. Zhu, Inhibition of SW620 human colon cancer cells by upregulating miRNA-145, World J. Gastroenterol. 22 (2016) 2771–2778, https://doi.org/10.3748/wjg.v22.i9.2771.
[54] A. González-Paredes, L. Sitia, A. Ruyra, C.J. Morris, G.N. Wheeler, M. McArthur, P. Gasco, Solid lipid nanoparticles for the delivery of anti-microbial oligonucleotides, Eur. J. Pharm. Biopharm. 134 (2019) 166–177, https://doi.org/10.1016/j.ejpb.2018.1.
[55] J. Crecente-Campo, S. Lorenzo-Abalde, A. Mora, J. Marzoa, N. Csaba, J. Blanco, Á. González-Fernández, M.J. Alonso, Bilayer polymeric nanocapsules: a formulation approach for a thermostable and adjuvanted E. coli antigen vaccine, J. Control. Release. 286 (2018) 20–32, https://doi.org/10.1016/j.jconrel.2018.07.018.
[56] M. Frattini, P. Saletti, F. Molinari, S. De Dosso, EGFR signaling in colorectal cancer: a clinical perspective, Gastrointest. Cancer Targets Ther. 5 (2015) 21, https://doi.org/10.2147/GICTT.S49002.
[57] J. Su, H. Liang, Y. Weiyan, N. Wang, S. Zhang, X. Yan, H. Feng, W. Pang, Y. Wang, X. Wang, Z. Fu, Y. Liu, C. Zhao, J. Zhang, C.-Y. Zhang, K. Zen, X. Chen, Y. Wang, MiR-143 and MiR-145 regulate IGF1R to suppress cell proliferation in colorectal cancer, PLoS ONE 9 (2014) 1–15, https://doi.org/10.1371/journal.pone.0114420.
[58] C. Yu, L. Tsai, M. Wang, C. Yu, W. Lo, Y.-C. Chang, G.-Y. Chiou, M.-Y. Chou, S.-H. Chiou, miR145 targets the SOX9/ADAM17 axis to inhibit tumor- initiating cells and IL-6 – mediated paracrine effects in head and neck cancer, Tumor Stem Cell Biol. 2 (2013) 3425–3440, https://doi.org/10.1158/0008-5472.CAN-12-3840.
[59] M. Zamani, M. Sadeghizadeh, M. Behmanesh, F. Najafi, Dendrosomal curcumin increases expression of the long non-coding RNA gene MEG3 via up-regulation of epi-miRs in hepatocellular cancer, Phytomedicine 22 (2015) 961–967, https://doi.org/10.1016/j.phymed.2015.05.071.
[60] H. Guo, Y. Xu, Q. Fu, Curcumin inhibits growth of prostate carcinoma via miR-208-mediated CDKN1A activation, Tumor Biol. 36 (2015) 8511–8517, https://doi.org/10.1007/s13277-015-3592-y.
[61] K. Pan, H. Chen, S.J. Baek, Q. Zhong, Self-assembled curcumin-soluble soybean polysaccharide nanoparticles: physicochemical properties and in vitro anti-proliferation activity against cancer cells, Food Chem. 246 (2018) 82–89, https://doi.

org/10.1016/j.foodchem.2017.11.002.
[62] S. Vicente, M. Peleteiro, J.V. Gonzalez-Aramundiz, B. Díaz-Freitas, S. Martínez-Pulgarín, J.I. Neissa, J.M. Escribano, A. Sanchez, Á. González-Fernández, M.J. Alonso, Highly versatile immunostimulating nanocapsules for specific immune potentiation, Nanomedicine 9 (2014) 2273–2289, https://doi.org/10.2217/nnm.14.10.
[63] C.-K. Chen, W.-C. Law, R. Aalinkeel, Y. Yu, B. Nair, J. Wu, S. Mahajan, J.L. Reynolds, Y. Li, C.K. Lai, E.S. Tzanakakis, S. a Schwartz, P.N. Prasad, C. Cheng, Biodegradable cationic polymeric nanocapsules for overcoming multidrug resistance and enabling drug-gene co-delivery to cancer cells, Nanoscale. 6 (2014) 1567–1572. doi: 10.1039/c3nr04804g.
[64] N. Skandrani, A. Barras, D. Legrand, T. Gharbi, H. Boulahdour, R. Boukherroub, Lipid nanocapsules functionalized with polyethyleneimine for plasmid DNA and drug co-delivery and cell imaging., Nanoscale. 6 (2014) 7379–90. doi: 10.1039/c4nr01110d.